Neuron, Vol. 23, 353–364, June, 1999, Copyright ©1999 by Cell Press

Destabilization of Cortical Dendrites and Spines by BDNF

Hadley Wilson Horch,*‡ Alex Krüttgen,† Stuart D. Portbury,*§ and Lawrence C. Katz*
*Howard Hughes Medical Institute
Department of Neurobiology
Duke University Medical Center
Durham, North Carolina 27710
†Department of Neurobiology
Stanford University School of Medicine
Stanford, California 94305

Summary

Particle-mediated gene transfer and two-photon microscopy were used to monitor the behavior of dendrites of individual cortical pyramidal neurons coexpressing green fluorescent protein (GFP) and brain-derived neurotrophic factor (BDNF). While the dendrites and spines of neurons expressing GFP alone grew modestly over 24–48 hr, coexpressing BDNF elicited dramatic sprouting of basal dendrites, accompanied by a regression of dendritic spines. Compared to GFP-transfected controls, the newly formed dendrites and spines were highly unstable. Experiments utilizing Trk receptor bodies, K252a, and overexpression of nerve growth factor (NGF) demonstrated that these effects were mediated by secreted BDNF interacting with extracellular TrkB receptors. Thus, BDNF induces structural instability in dendrites and spines, which, when restricted to particular portions of a dendritic arbor, may help translate activity patterns into specific morphological changes.

Introduction

A neuron's dendritic architecture determines the nature of its inputs and its role in neuronal circuitry (e.g., Eysel, 1982; Friedlander et al., 1982; Bacon and Murphey, 1984). Dendritic development initially follows genetic dictates (Bartlett and Banker, 1984a) but can be modified by levels and patterns of activity (Bartlett and Banker, 1984b) in both developing (e.g., Volkmar and Greenough, 1972; Katz and Constantine-Paton, 1988; Kossel et al., 1995; Segal, 1995) and mature systems in response to numerous manipulations, including denervation (Parnavelas et al., 1974), long-term potentiation (LTP) (Van Harreveld and Fifkova, 1975; Buchs and Muller, 1996; but see Sorra and Harris, 1998), or environmental stimulation (e.g., Comery et al., 1996; Jones et al., 1997).

However, the molecular signals that transduce the effects of activity remain obscure. The neurotrophin family of growth factors (reviewed by McAllister et al., 1999), and in particular brain-derived neurotrophic factor (BDNF), are particularly attractive candidates for mediating the effects of activity on morphology since their expression (Castren et al., 1992) and release (Goodman et al., 1996) are, at least in part, activity dependent, and since they alter dendritic morphology (reviewed by McAllister et al., 1999). BDNF influences ocular dominance column development and plasticity (Cabelli et al., 1995; Galuske et al., 1996), spine density in Purkinje cell cultures (Shimada et al., 1998), and initial dendritic outgrowth in neocortex (McAllister et al., 1996).

Dendritic plasticity has usually been examined in dissociated cell cultures, where activity levels are abnormally low, or experiments have relied on population data collected at single time points to extrapolate the dynamic behavior of single cells. Furthermore, conventional experimental approaches have delivered factors by bath application, which may cause numerous indirect effects. To overcome these limitations, we combined particle-mediated gene transfer and two-photon microscopy (Denk et al., 1990) in cortical slices to repeatedly image individual neurons transfected with GFP alone or cotransfected with the gene for BDNF or NGF. This allowed following the behavior of individual BDNF-overexpressing neurons over time and comparing their behavior to control neurons under the same conditions. While control neurons in slices had stable dendrites and modest changes in dendritic spines over 24–48 hr, dendrites from BDNF-overexpressing neurons underwent massive sprouting. Moreover, BDNF overexpression profoundly destabilized dendritic spines, leading to their almost complete disappearance. Thus, BDNF may induce local dendritic instability that allows activity-dependent morphological changes in juvenile and adult animals.

Results

To visualize neurons within cortical slices, we transfected individual neurons with GFP using particle-mediated gene transfer, or biolistics (see Experimental Procedures). This technique yielded hundreds of transfected neurons per slice where individual dendritic arbors could be easily visualized (Lo et al., 1994). Reliable cotransfection with biolistics was easily achieved simply by coating gold particles with various mixtures of DNAs encoding BDNF, NGF, or GFP. We employed epitope-tagged BDNF and NGF constructs (BDNF-myc and NGF-myc) whose expression could be visualized with post hoc immunohistochemistry. We compared the morphology of GFP control neurons to those cotransfected with GFP and BDNF or GFP and NGF in layer 2/3 pyramidal neurons of ferret primary visual cortex at postnatal days (P) 25–28. By these ages, neurons have established much of their mature morphology. Although P27 is ~1 week prior to eye opening, cortical networks are sufficiently complex to support visual responses such as orientation selectivity (Ruthazer and Stryker, 1996). This stage is considerably later than that of previous work by McAllis-

‡To whom correspondence should be addressed (e-mail: hwilson@neuro.duke.edu).
§Present address: Cogent Neuroscience, 710 West Main Street, Durham, North Carolina 27701.

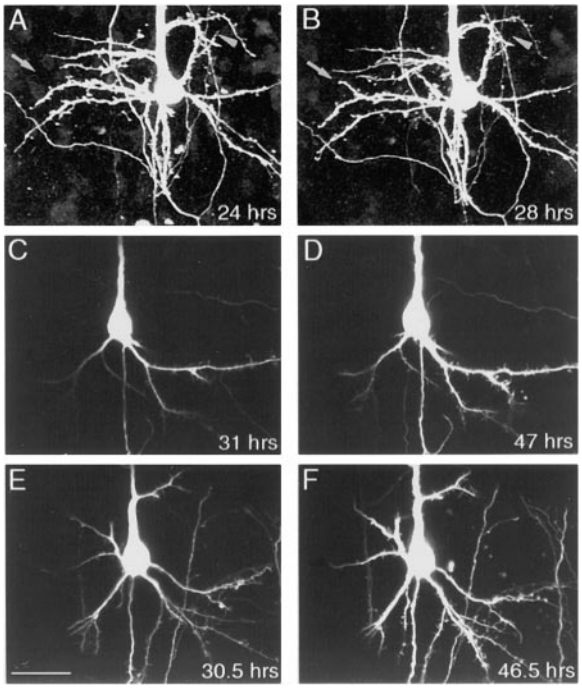

Figure 1. Two-Photon Time-Lapse Images Indicate that Dendrites on GFP-Transfected Pyramidal Neurons in Visual Cortex Slices Are Stable over Time

(A and B) Layer 6 pyramidal neuron (projection of 40 optical sections) imaged 24 hr after transfection (A) and 4 hr later (B). Arrows indicate dendritic growth over time, and arrowheads note retraction.

(C and D) Layer 2/3 pyramidal neuron (projection of 20 optical sections) imaged 31 hr after transfection (C) and 16 hr later (D). Although the intensity of the GFP label increased over this interval, almost all of the morphological features seen in (C) are visible in (D).

(E and F) Layer 2/3 pyramidal neuron (projection of 22 optical sections) imaged 30.5 hr after transfection (E) and 16 hr later (F). In addition to the stability of the dendrites, thin, stable axonal processes can be seen to the right of the cell body in both images. Scale bar, 25 μm.

ter et al. (1995), which described the effects of bath-applied neurotrophins on the initial dendritic outgrowth of immature layer 4 neurons (P14).

Stability of Control Dendrites and Spines

The dendrites of cortical pyramidal neurons transfected with GFP alone were remarkably stable over 4–17 hr (Figure 1). Pyramidal neurons exhibited morphological characteristics typical of these cells in vivo, including three to five prominent basal dendrites, each of which branched two to three times. The overall number and arrangement of basal dendrites changed little over time, and individual neurons were easily identified when imaged repeatedly. Although large-scale morphological changes were not seen, these neurons were not static, since dendrites grew and retracted, especially at their tips (e.g., Figures 1A and 1B). Ten time-lapse pairs were analyzed quantitatively. Control neurons averaged 3.7 ± 0.2 primary basal dendrites at the first imaging session (24 hr posttransfection); this increased slightly to 4.0 ± 0.2 dendrites 16 hr later (not a statistically significant increase). In seven of ten cells, no new basal dendrites appeared over this time interval, whereas three of ten neurons each gained one new dendrite.

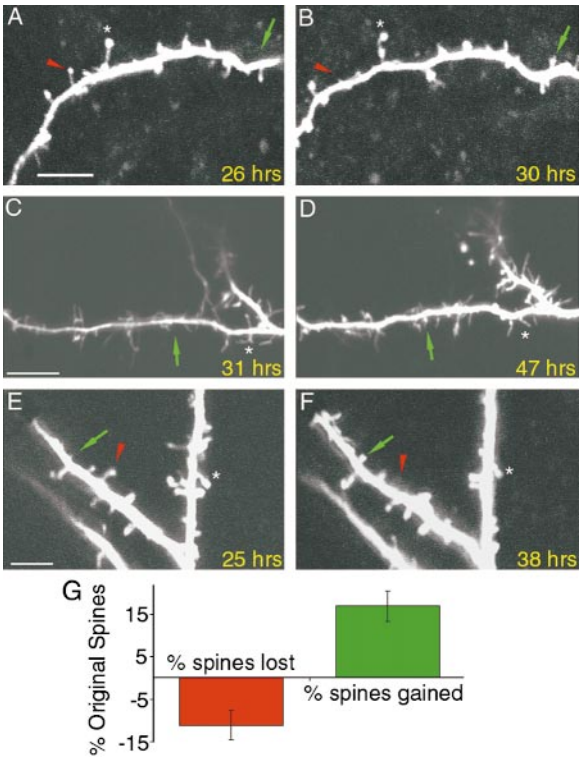

Figure 2. Two-Photon Time-Lapse Images Reveal Loss and Gain of Spines over Time

The spine population consists mainly of thin spines but also includes long dendritic filopodia (5–10 μm) and short stubby spines. Red arrowheads indicate spines lost, and green arrows indicate spines gained. Asterisks mark examples of spines that exhibit morphological changes over time. Scale bars, 10 μm.

(A and B) Image of a dendritic stretch with spines (projection of 12 optical sections) from a GFP-transfected neuron taken 26 hr after transfection (A) and 4 hr later (B).

(C and D) Image of a dendritic stretch with spines (projection of 9 optical sections) from a GFP-transfected neuron taken 31 hr after transfection (C) and 16 hr later (D).

(E and F) Image of a dendritic stretch with spines (projection of 18 optical sections) from a GFP-transfected neuron taken 25 hr after transfection (E) and 13 hr later (F).

(G) Quantification of the percentage of spines lost (red bars) or gained (green bars) over 16 hr (n = 6 dendritic sections each from different neurons, 142 spines were analyzed, mean ± SEM).

In contrast to the stability of basal dendrites, dendritic spines showed considerably more flux. Spines (defined as processes ≤3 μm long) were both motile and unstable (Figure 2). During 16 hr time periods, a significant population of new spines appeared (17% of original spine number); during the same period, 11% of the spines originally present were lost (Figure 2G). Most spines (89%) were recognizable after 4–16 hr even though some had undergone minor changes in shape or altered their orientations with relation to the dendritic shaft (Figures 2A, 2B, 2E, and 2F).

BDNF Overexpression Rapidly Alters Dendritic Architecture

The cotransfection capability of particle-mediated gene transfer allows creation of chimeric tissues in which a small population of transfected neurons resides in a

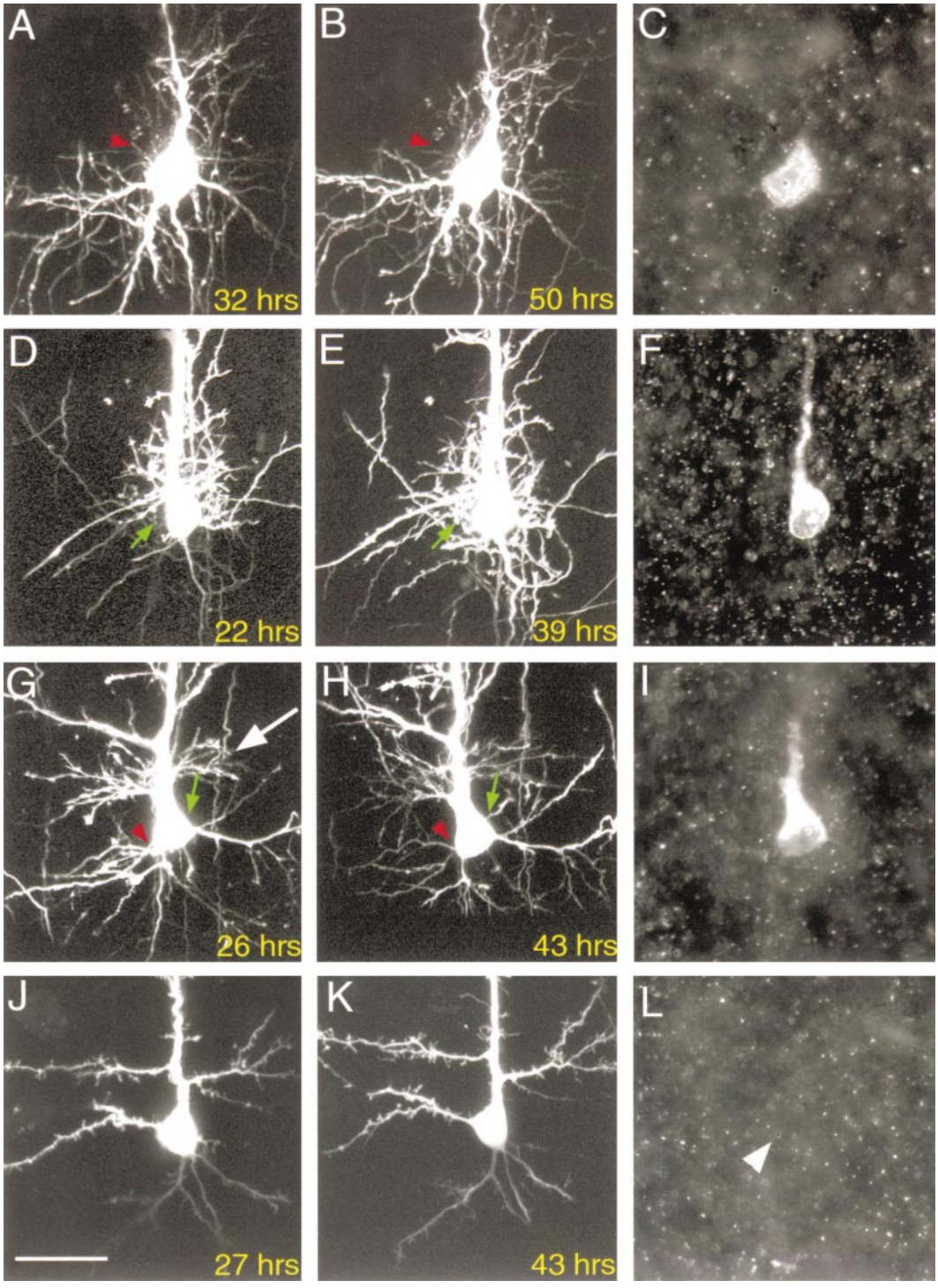

Figure 3. BDNF Overexpression Profoundly Alters the Architecture of Neurons by Inducing a Halo of New Basal Dendrites

Two-photon images of living neurons taken at two different points in time illustrate the development and growth of dendrites. Note the thicker, branched dendrites underlying the halo of short, fine processes. Red arrowheads mark dendrites lost and green arrows mark dendrites gained over the 16 hr time course.

(A and B) Neuron cotransfected with BDNF and GFP (projection of 18 optical sections) taken 32 hr after transfection (A) and 18 hr later (B).

(C) Immunohistochemistry from the neuron in (A) and (B) for the myc epitope tag shows BDNF expression.

(D and E) Neuron cotransfected with BDNF and GFP (projection of 24 optical sections) taken 22 hr after transfection (D) and 17 hr later (E).

(F) Immunohistochemistry from the neuron in (D) and (E) for the myc epitope tag shows BDNF expression.

(G and H) Neuron cotransfected with BDNF and GFP (projection of 26 optical sections) imaged 26 hr after transfection (G) and 17 hr later (H). White arrow in (G) indicates sprouting of dendrites from the proximal portion of the apical dendrite.

(I) Immunohistochemistry from the neuron in (G) and (H) for the myc epitope tag shows BDNF expression.

(J and K) Neuron transfected with GFP alone (projection of 26 optical sections) shows normal dendritic architecture 27 hr after transfection (J) and 16 hr later (K).

(L) Immunohistochemistry from the neuron in (J) and (K) for the myc epitope tag shows a complete lack of BDNF expression. White arrowhead indicates gold particle in the nucleus of the GFP-transfected neuron.

Scale bar, 25 μm.

matrix of normal cells. Overexpression of epitope-tagged BDNF in individual layer 2/3 pyramidal neurons profoundly altered dendritic architecture. Unlike the basal dendritic arbors of control neurons, which were comprised of three to four primary branched dendrites, each about 75 μm long, BDNF-transfected neurons exhibited a prominent halo of short, unbranched basal dendrites (Figure 3). Numerous short, fine dendrites sprouted from the proximal portion of the apical dendrite as well (Figure 3G), a phenotype rarely observed in control neurons. In addition to the halo of short, unbranched dendrites, three to four thicker, branched dendrites, similar to dendrites of control neurons, were also observed; these were probably the original basal dendrites already present prior to transfection (Figure 3).

These qualitative impressions were confirmed by quantitation of basal dendrites from two-photon images of control and BDNF-transfected neurons taken 24 hr after transfection. Compared to the 3.7 ± 0.2 basal dendrites in controls (see above), BDNF-transfected neurons had 12 ± 1.3 processes ($n = 14$, range 6–24), a 324% increase ($p < 0.001$; see Experimental Procedures for quantitation criteria). Post hoc immunohistochemistry confirmed that, in all cases, these neurons expressed the epitope-tagged BDNF protein (Figure 3, right column).

To confirm the results obtained from time-lapse pairs, Sholl analysis was used on a larger population to assess dendritic complexity (Sholl, 1953; see Experimental Procedures). This analysis revealed that BDNF overexpression increased the number of short, unbranched processes while reducing somewhat the higher-order branching of the original basal dendritic architecture, findings consistent with analysis of the time-lapse images. The number of processes in the first 40 μm from the cell body (corresponding to the first four rings of the Sholl analysis) increased significantly in neurons overexpressing BDNF relative to controls (Figure 4A; $p < 0.05$). BDNF also reduced the number of higher-order branches in the basal dendrites already present, as seen in the statistically significant decrease in intersections between 70 and 90 μm from the cell body (Figure 4A; $p < 0.05$). Examining the number of intersections on the first ring (20 μm diameter circle centered on the cell body), which quantifies the number of basal dendrites, enables comparison of this population data with the quantitation of the basal dendrites in the two-photon images. Using this modification of the Sholl analysis, we observed a 2.4-fold increase in basal dendrites in BDNF-overexpressing neurons relative to controls, a difference that is highly significant ($p < 0.001$) and comparable to the 3.2-fold increase detected in the time-lapse pairs analyzed with two-photon microscopy.

Time-lapse studies always began at least 24 hr after transfection, in order to allow sufficient filling with GFP, which ensured the detection of all processes (see Experimental Procedures). To follow the emergence of the BDNF-induced halo beginning at earlier times, anti-GFP immunohistochemistry following fixation was used to greatly amplify the GFP signal. Using the modified Sholl analysis described above, we counted the number of basal dendrites beginning at 18 hr, the earliest time at which amplified GFP filling was complete, and continuing at 24, 40, and 52 hr (Figure 4B). While the number

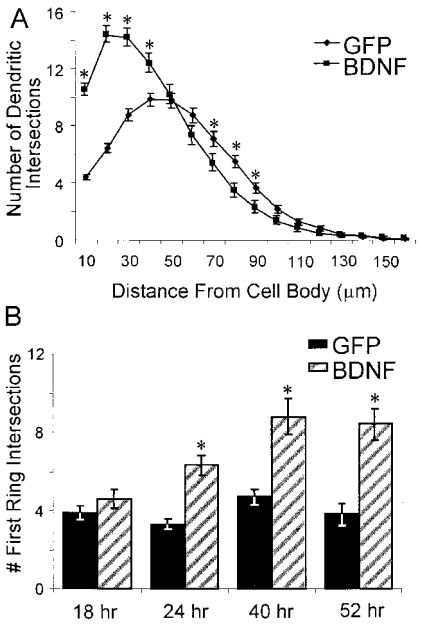

Figure 4. The Effects of BDNF Overexpression on Populations of Neurons Confirm Results from Time-Lapse Studies

(A) Sholl analysis results for GFP-transfected ($n = 60$, diamonds) and GFP- and BDNF-cotransfected neurons ($n = 60$, squares) show the branching of basal dendrites with increasing distance from the cell body. BDNF induced a significant increase in the number of short processes within 40 μm of the cell body as compared to control neurons. In addition, BDNF elicited a decrease in higher-order branches in an area 70–90 μm from the cell body. Repeated measures ANOVA on all rings shows there is an interaction of treatment by ring ($p < 0.001$), and Student's t test on a per ring basis indicates statistically significant effects of treatment (asterisk indicates $p < 0.05$, mean ± SEM for each ring).

(B) The BDNF-induced halo develops rapidly, reaching steady state between 40 and 52 hr after transfection. Values for GFP-transfected neurons (black bars) were equivalent at all time points, whereas BDNF-transfected neurons (striped bars) had already significantly increased their number of basal dendrites by 24 hr after transfection (ANOVA group difference, $p < 0.001$; Tukey multiple comparison posttest, asterisk indicates $p < 0.05$ as compared to GFP; $n = 10$; mean ± SEM).

of control basal dendrites remained constant, BDNF-overexpressing neurons showed significant increases over controls as early as 24 hr posttransfection ($p < 0.05$). These halos continued to increase in density over the next 22 hr, reaching an asymptote between 40 and 52 hr. Thus, time-lapse images initiated 24 hr after transfection captured the ongoing development of this dendritic halo, and our comparison of basal dendrite number between GFP- and BDNF-overexpressing neurons at 24 hr was a conservative estimate of the effects of BDNF.

BDNF Alters the Stability of Dendrites and Spines

BDNF not only induced the formation of a new population of short dendrites but also greatly decreased the stability of existing dendrites. Repeated imaging of individual dendrites with the two-photon microscope allowed us to follow the structure of individual dendrites over many hours. Both the newly formed dendrites in the halo, as well as the longer, branched dendrites were

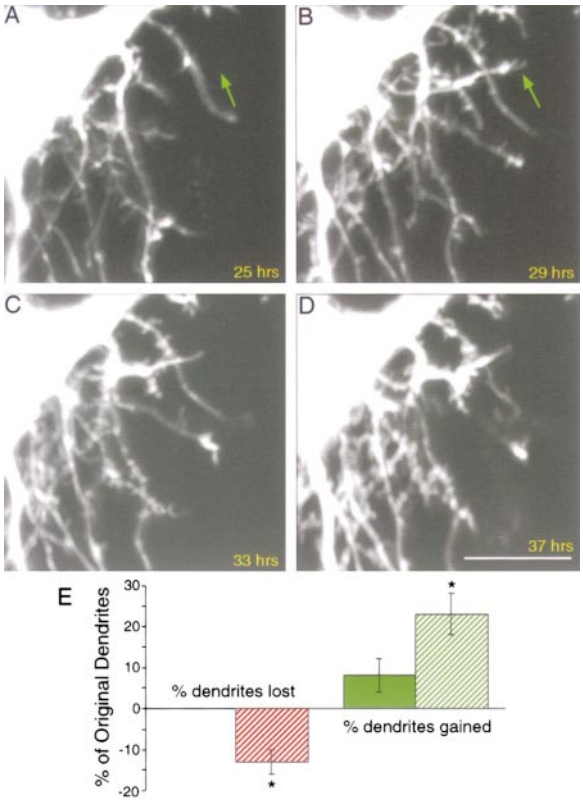

Figure 5. High-Power View of the BDNF Overexpression–Induced Halo Shows Rapid Alterations in Dendritic Architecture

(A–D) Neuron cotransfected with BDNF and GFP (projection of 10 optical sections) imaged 25 hr (A), 29 hr (B), 33 hr (C), and 37 hr (D) after transfection. Green arrows in (A) and (B) indicate a dendrite that appears de novo and elongates dramatically within 4 hr. Note the small changes in individual dendrites that occur over this time. Scale bar, 10 μm.

(E) Comparison of the behavior of dendrites on GFP (n = 10, solid bars) and BDNF-overexpressing neurons (n = 14, striped bars). BDNF overexpression caused statistically significant increases in the percentage of dendrites that are lost and added as compared to controls over the 16 hr time period examined (asterisk indicates $p < 0.05$, Student's t test, mean ± SEM).

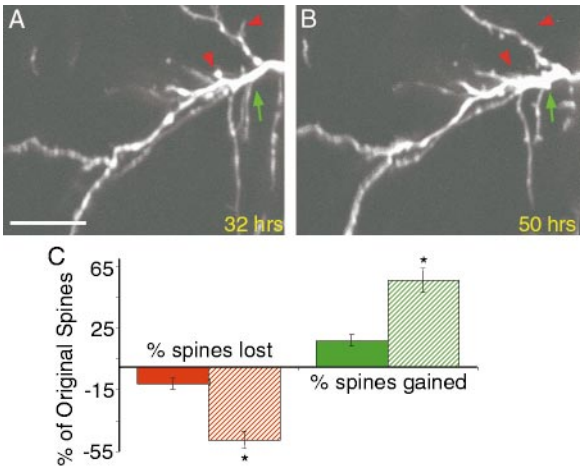

Figure 6. BDNF Overexpression Alters the Density and Stability of Spines

(A and B) Portion of a dendrite (projection of 8 optical sections) from a neuron cotransfected with BDNF and GFP imaged 32 hr after transfection (A) and 18 hr later (B). Red arrowheads indicate spines that were lost, and the green arrow indicates a spine that emerged over time. Scale bar, 10 μm.

(C) BDNF overexpression changes the stability of existing spines. Spines from BDNF-transfected neurons (n = 6 cells, 30 spines, striped bars) differed significantly from control neurons (n = 6 cells, 142 spines, solid bars) in the percentage of spines lost as well as in the percentage of spines gained (asterisk indicates $p < 0.05$, Student's t test, mean ± SEM).

much less stable than controls, although these instabilities were manifested differently.

Time-lapse images revealed numerous examples of dendrites in the halos that were lost and gained over time (Figure 3, arrows), while Sholl analysis indicated that distal branches were lost in response to BDNF overexpression (see above); both of these observations contrast with the morphology and overall dendritic stability observed in control neurons. The dendritic stability of BDNF-overexpressing neurons was also monitored at shorter (4 hr) intervals (Figure 5). In addition to the gain or loss of individual primary basal dendrites (Figures 5A and 5B), dendritic processes moved about in the space surrounding the cell body. In 14 time-lapse pairs, dendritic turnover was quantified after a 16 hr interval (Figure 5E). While control neurons never lost basal dendrites, 13% ± 3% of the original dendrites that composed the halo of the BDNF-overexpressing neurons were lost ($p \leq 0.001$). Similarly, control neurons rarely added new dendrites (8% ± 4%), whereas neurons overexpressing BDNF increased the number of dendrites by 23% ± 5% ($p < 0.05$).

Although the original branched dendrites present on neurons overexpressing BDNF remained intact, BDNF overexpression greatly reduced the density and stability of the few remaining spines on these dendrites (Figures 6A and 6B). Based on quantitative analysis of two-photon images, control dendrites had 2.1 ± 0.3 spines/10 μm of dendrite, whereas neurons overexpressing BDNF had 0.9 ± 0.4 spines/10 μm of dendrite ($p = 0.022$). This nearly 2.5-fold decrease in spine density indicated that BDNF-overexpressing neurons lost one of the hallmarks of mature excitatory synapses.

The few spines that remained on the dendrites of BDNF-overexpressing neurons were transient. While 89% ± 3% of the control spines were recognizable after 16 hr, only 53% ± 6% of the spines on BDNF-overexpressing neurons could be detected 16 hr later. This decrease in spine retention reflects an increase in the percentage of spines lost (11% ± 3% for controls versus 48% ± 6% for BDNF-overexpressing neurons, $p < 0.001$; Figure 6C). In addition, BDNF-overexpressing neurons added new spines at a greater rate than control neurons ($p = 0.001$; Figure 6C), suggesting that these dendrites could potentially change or add synaptic partners at a greater rate than control neurons.

BDNF Acts through an Autocrine Loop

BDNF is thought to be released under specific conditions from neurons (Goodman et al., 1996) into the extracellular space. To determine whether BDNF was acting directly and specifically on the cotransfected neurons

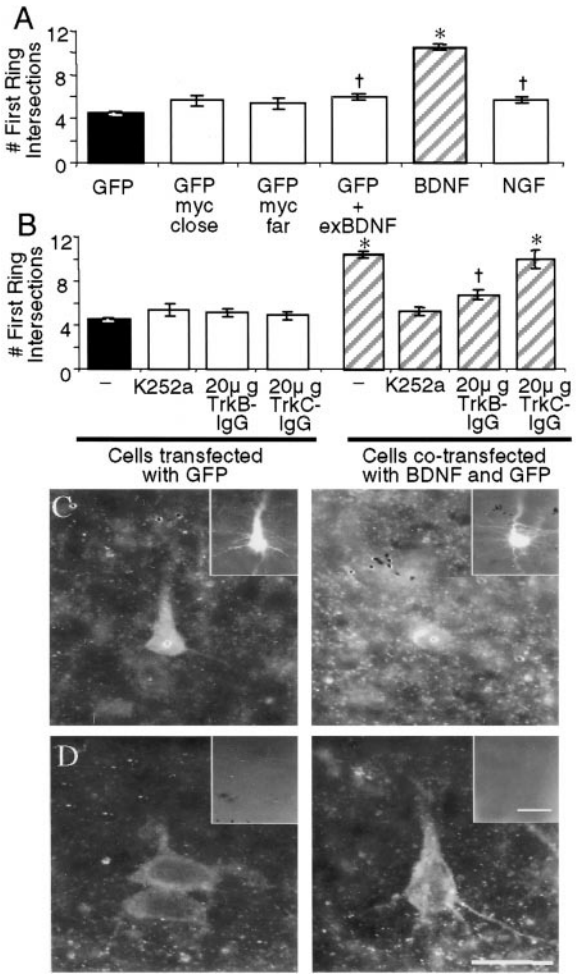

Figure 7. BDNF Acts Autonomously via Extracellular Trk Receptors to Alter Dendritic Morphology

(A) Dual gold experiments (see text) reveal that GFP-transfected cells neither close to (GFP myc close, n = 15) nor far from (GFP myc far, n = 15) BDNF-myc-transfected neurons showed significant increases in the number of basal dendrites as compared to GFP-transfected neurons (n = 105, 60 of which are from first ring data of Figure 4A, $p > 0.05$). Overexpression of NGF did not increase basal dendrites to the same extent as BDNF, although these neurons showed a slight increase in the number of basal dendrites compared to GFP neurons (n = 90, cross indicates $p < 0.01$). Addition of exogenous BDNF (200 ng/ml) to GFP-transfected neurons (GFP + exBDNF, n = 57) also induced a slight significant increase in the number of basal dendrites relative to controls ($p < 0.01$, mean ± SEM). (B) Addition of either 200 nM K252a (n = 30) or 20 μg TrkB-IgG (n = 30) to BDNF-overexpressing neurons significantly reduced the effects of BDNF overexpression (n = 95) on primary basal dendrites (asterisk indicates values significant at $p < 0.01$ as compared to all other groups). TrkB-IgG (20 μg) treatment did not reduce the number of primary basal dendrites on neurons overexpressing BDNF completely to control levels (cross indicates $p < 0.01$). Treating GFP-transfected neurons with 20 μg TrkB-IgG did not affect primary dendritic number (n = 30). Finally, 20 μg TrkC-IgG treatment did not alter the number of primary basal dendrites on GFP neurons (n = 15) nor on BDNF-overexpressing neurons (n = 15). ANOVA ($p < 0.001$) followed by a Tukey posttest revealed that neurons overexpressing BDNF (n = 95, 60 of which are from first ring data of Figure 4A) were significantly different from all others (asterisk indicates $p < 0.01$, cross indicates values statistically different from those for GFP neurons [$p < 0.01$] but not from the dual gold values, mean ± SEM).

themselves, or indirectly through actions on neighboring neurons, we examined the dendritic arbors of GFP-transfected neurons in slices that also contained BDNF-transfected neurons. In addition, we examined the arbors of neurons overexpressing NGF-myc or exposed to bath-applied exogenous BDNF, TrkB, and TrkC receptor bodies or K252a, an inhibitor of tyrosine kinases.

In the first set of experiments, we transfected individual slices with two separate kinds of gold particles: one coated with cDNA for BDNF-myc alone, and the other coated with GFP alone. These "dual gold" experiments (see Experimental Procedures) produced slices in which one population of neurons was transfected with BDNF-myc only, while a second, nonoverlapping, population of neurons was transfected with GFP alone. In fixed slices, we examined the morphology of GFP-expressing neurons that were located close to (<20 μm) or far from (>50 μm) neurons overexpressing BDNF, as identified by the myc tag. If BDNF released from transfected neurons was acting in a paracrine manner, then GFP-transfected neurons close to a BDNF-expressing neuron should either grow preferentially toward the neuron or exhibit a dendritic halo, while GFP-labeled neurons far from BDNF-transfected neurons should not be affected. Analysis of these two populations of GFP-transfected neurons indicated that the proximity of a BDNF source did not differentially affect the number of primary basal dendrites (Figure 7A). In fact, the dendritic arbors of GFP-transfected neurons in these "dual gold" slices did not differ significantly from controls.

These results suggest that BDNF overexpression–induced changes in dendritic arbors are mediated principally through an autocrine loop. In support of this conclusion, GFP-transfected neurons in slices treated with 200 ng/ml BDNF showed only a small (although statistically significant) increase in the number of basal dendrites as compared to GFP-transfected neurons (Figure 7A; $p < 0.01$). Clearly, bath-applied exogenous BDNF did not reproduce the effects of overexpressing BDNF in single neurons.

The effects of BDNF overexpression on dendritic morphology are not simply the consequences of overexpressing neurotrophins in general. Overexpression of another neurotrophin, NGF-myc, only slightly increased the number of primary basal dendrites (Figure 7A; $p < 0.01$) compared to neurons transfected with GFP. However, NGF-overexpressing neurons had significantly fewer basal dendrites as compared to neurons overexpressing BDNF (Figure 7A; $p > 0.05$), and expression of this neurotrophin neither induced a halo nor eliminated dendritic spines.

(C) Anti-BDNF immunohistochemistry of two layer 2/3 neurons co-transfected with BDNF and GFP. Cells in insets are visualized with anti-GFP immunohistochemistry. Anti-BDNF immunoreactivity can be seen in the cell body, in the proximal portion of the apical dendrite, and in the basal dendrites.

(D) Anti-BDNF immunohistochemistry of two untransfected layer 5 neurons. Inset shows lack of label after anti-GFP immunohistochemistry. Note the similarity in the pattern of the anti-BDNF immunoreactivity between the layer 2/3 transfected neurons and the layer 5 untransfected neurons.

Scale bars, 25 μm.

To determine whether BDNF was acting in a true autocrine fashion, TrkB receptor bodies (TrkB-IgGs), which specifically chelate TrkB ligands (Shelton et al., 1995), were added to the medium. Culturing slices containing BDNF-overexpressing neurons in the presence of 20 μg/ml TrkB-IgG almost completely eliminated the halo. Neurons overexpressing BDNF had 10.5 basal dendrites, which were reduced to 6.7 after 36 hr of TrkB-IgG exposure (Figure 7B; $p < 0.01$). TrkB-IgG did not affect the number of primary basal dendrites on GFP-transfected neurons (Figure 7B; $p > 0.05$); however, it did increase the number of secondary branches, causing an increase in the branching of dendrites between 60 and 100 μm from the cell body (unpublished data). To further demonstrate that the observed effects of overexpression were due to BDNF and TrkB activation, 20 μg/ml of TrkC receptor body, which specifically chelates neutorophin-3 (NT-3), was added to control slices and slices containing BDNF-overexpressing neurons. In contrast to the marked effect of TrkB receptor bodies, neither 20 μg/ml (Figure 7B) nor even 100 μg/ml TrkC-IgG (data not shown) affected the extent of the halo in BDNF-overexpressing neurons or the number of primary dendrites of cells transfected with GFP alone.

To confirm that the effects seen in BDNF-overexpressing neurons resulted from activation of Trk receptors, we treated slices with K252a, a drug which blocks Trk receptor activation by neurotrophins (Berg et al., 1992; Tapley et al., 1992) and the physiological effects of neurotrophins (Kang and Schuman, 1995). Culturing slices in the presence of 200 nM K252a blocked the BDNF-induced morphological effects on primary basal dendrites (Figure 7B; $p < 0.01$) but had no effect on the primary dendrites of control neurons (Figure 7B; $p > 0.05$).

Finally, there is always a concern in an overexpression paradigm that the levels of the transfected protein are completely nonphysiological. To address this, an anti-BDNF-specific antibody was used to visualize the BDNF protein and quantitate the relative levels of BDNF in transfected and nontransfected neurons within the same slice. Although BDNF levels in transfected neurons were higher than those found in other layer 2/3 neurons (Figure 7C), these levels were similar to levels seen in untransfected layer 5 cells (Figure 7D). Quantifying the anti-BDNF immunohistochemistry revealed corrected gray values ranging from 158 to 654 units for untransfected layer 5 neurons ($\bar{x} = 446 \pm 59$ units, $n = 10$) and from 172 to 640 units for transfected layer 2/3 neurons ($\bar{x} = 456 \pm 82$ units, $n = 5$, Student's t test, $p = 0.925$) within the same slice reacted under identical conditions. The pattern of immunoreactivity (IR) was also similar between the two different types of neurons. Both had large amounts of BDNF-IR in the cell body, with less intense BDNF-IR in the proximal portion of the apical and basal dendrites. We can conclude from these results that BDNF acts predominantly in an autocrine fashion as demonstrated by the almost complete blockade of the BDNF-induced halo by TrkB-IgG and K252a, and by the different magnitude of morphological effects induced by exogenous BDNF. Further, the actions of BDNF are specific and not simply due to overexpression of a neurotrophin, since neurons transfected with NGF did not grow halos or lose spines.

Discussion

These results demonstrate that under normal conditions dendrites are stable over many hours and that remodeling occurs predominantly at the level of spines. BDNF overexpression alters and destabilizes normal dendritic morphology and augments spine remodeling. Neurons overexpressing BDNF undergo a significant increase in the number of basal dendrites and a marked reduction in their stability.

Differential Stability of Dendritic Architecture and Spines

In the neocortex, dendritic development begins with the de novo formation of basal dendrites capped by dendritic growth cones. As development continues, the rapid initial outgrowth phase slows, spine formation begins shortly after thalamic afferents arrive, dendritic growth cones disappear, and dendrites approach their mature form (Miller, 1988). The postnatal ferrets used in these experiments had not opened their eyes; however, pyramidal cell dendrites in layer 2/3 of the visual cortex were nearing their mature form. Imaging these neurons over time revealed stable dendritic arbors and few dendritic growth cones. In addition, many of the spines present were in mature form and the population was not dominated by the stubby spines (Harris et al., 1992) or dendritic filopodia (Ziv and Smith, 1996) indicative of immature dendrites.

Two-photon microscopy revealed that dendritic architecture changed slowly over the time periods examined, with most changes confined to the growth or retraction of individual dendritic tips. These observations are consistent with the stability of dendrites imaged in P12–P14 slices of rat hippocampus (Dailey and Smith, 1996) and with the eventual slowing of tectal dendritic growth seen during tadpole development (Wu and Cline, 1998).

The stability of dendrites, however, does not imply that the overall dendritic morphology remained static. Indeed, spines—where a majority of the excitatory synaptic connections are made—were unstable. Using a conservative length estimate to define spines (see Experimental Procedures), we saw both gain of individual spines and loss of the original population over 16 hr; in addition, spines frequently changed their size and shape. Although there have been many suggestions of such alterations in spine morphology after induction of LTP (e.g., Fifkova and Delay, 1977; Desmond and Levy, 1986; but see Sorra and Harris, 1998), after synaptic activation (Maletic-Savatic et al., 1999), or following environmental stimulation or training (e.g., Comery et al., 1996; Jones et al., 1997), few experiments (see below) have reported morphological changes in spines under normal conditions and in individual neurons.

Spines may not normally be stable over time, but instead may "twitch" in response to activity (Crick, 1982), and recent evidence shows that spines can alter their shapes rapidly (Fischer et al., 1998) and even appear and disappear over time (Hosokawa et al., 1992; Dailey and Smith, 1996; Maletic-Savatic et al., 1999). Fischer et al. (1998) recently reported extremely rapid, actin-dependent changes in the shape (but not size) of dendritic spines in dissociated hippocampal cultures, indicating that spines may be less stable than widely

thought. Our results indicate that at least a subset of spines are not stable fixtures on the dendrites in a slice, since they are lost and gained over time and can change shape. Layer 2/3 neurons receive input from layer 4 neurons as well as other layer 2/3 neurons, and these inputs remain largely intact in slice preparations. Shorter-term, repeated imaging experiments would allow a more in depth examination of changes in spine morphology in slices over time, including estimates of average spine lifetimes and measurements of movements, although preliminary observations with short imaging interludes suggest that rapid changes do not occur in this population.

BDNF Alters the Morphology and Maintenance of Dendrites and Spines

BDNF overexpression greatly altered the morphology of dendrites and spines. The largest effect was on the number of basal dendrites, which increased by 324% over control neurons and were so numerous that they formed a halo around the cell body. BDNF overexpression also dramatically altered the density and stability of spines and resulted in neurons with 57% fewer spines than controls. The effects of BDNF were not restricted to the basal dendrites, however, since we observed an increased number of dendrites that had sprouted from the proximal portion of the apical dendrite. Although not quantified, there were no obvious changes in the distal stretches of the apical dendrites.

Since the majority of excitatory synapses are normally found on spines, and since spine density in the visual cortex increases as the visual system matures (Lund et al., 1977; Bourgeois and Rakic, 1993), the decreased density and stability of existing spines on neurons overexpressing BDNF indicates that these dendrites may have lost a significant proportion of their excitatory input. It is possible that the excitatory synapses are not actually lost but are simply transferred onto the dendritic shaft. Since the role of spines in synaptic physiology is unclear (reviewed by Shepherd, 1996), the cellular consequences of this morphological alteration are difficult to predict. Considering the increased mobility and turnover of the dendrites in the halo as well as the elevated loss of spines, it appears likely that the entire dendritic architecture of these BDNF-overexpressing neurons is significantly destabilized.

The ability to create individual transgenic neurons within a normal slice is one of the major advantages of particle-mediated gene transfer. Single-cell transfection, unlike bath application of proteins or drugs, does not affect the entire network. Our results clearly show that overexpression of BDNF has a distinct effect that cannot be mimicked by bath application or even by a nearby point source of BDNF (see below), indicating that altering the local BDNF concentration and the level of Trk receptor activation within one neuron has a unique effect on the morphology of that neuron. At these ages in cortex, the levels of truncated TrkB receptors on neurons and glia are beginning to rise dramatically (Allendoerfer et al., 1994), which may lead to sequestration or internalization of a large amount of BDNF (Biffo et al., 1995; Fryer et al., 1997). We suspect that the retrograde release of BDNF from the dendrites of transfected neurons may overcome the chelating effects of truncated receptors and allow activation of the full-length TrkB still present on these neurons. The observation that the presence of a nearby source of BDNF from a transfected neuron failed to alter dendritic arbors suggests that the range of action of released BDNF may by quite low, perhaps on the order of only a few micrometers.

Alternatively, BDNF could have induced the observed effects on neuronal morphology via an intracellular mechanism, which is not dependent upon secretion of BDNF into the extracellular space. This is unlikely, since myc-tagged neurotrophins have been characterized, are known to be released from neuroendocrine cells, and are capable of inducing Trk receptor phosphorylation (Möller et al., 1998). However, the situation may be different in pyramidal neurons growing within a cultured slice. Although culturing slices in the presence of K252a blocked the effects of BDNF overexpression (Figure 7B), this does not distinguish between BDNF acting extra- versus intracellularly, since K252a is lipophilic and binds to the intracellular portion of the Trk receptor (Kase et al., 1986; Tapley et al., 1992). However, the action of BDNF is almost entirely through extracellular TrkB receptors since TrkB-IgG, which does not pass through cell membranes, blocked the formation of the dendritic halo. The observation that TrkB-IgG did not completely reduce the number of primary basal dendrites to control levels may be a consequence of some intracellular actions of BDNF; alternatively, the concentration of extracellular BDNF-myc may locally have exceeded the binding capabilities of the TrkB-IgG added. It is also unlikely that BDNF acts inside the cell prior to being secreted, as activation of overexpressed TrkB receptors causes a similar halo of basal dendrites in layer 6 neurons (T. Yacoubian and D. Lo, personal communication).

The fact that K252a does not affect the number of primary basal dendrites on GFP-transfected control neurons at first appears problematic and could be interpreted to mean that endogenous neurotrophins are not regulating dendritic morphology at this age. However, based on previous work by McAllister at al. (1995, 1997), two different endogenous neurotrophins can exert opposite effects within each cortical layer, and blocking one can unmask the influence of the second. Since K252a indiscriminately blocks all Trk receptors, none of the endogenous neurotrophins would be able to influence dendritic morphology in the presence of K252a. Consistent with this, blocking endogenous BDNF with TrkB-IgG induces an increase in the number of secondary dendritic branches in an area 60–100 μm from the cell body. This coincides almost exactly with the significant decrease in dendritic branching observed in BDNF-overexpressing neurons between 70 and 90 μm from the cell body (Figure 4A), and indicates that endogenous BDNF influences dendritic branching within this area under normal circumstances.

Finally, the fact that cells cotransfected with GFP and NGF showed only modest increases in the number of basal dendrites indicates that the actions of BDNF are largely specific. Since neither TrkA nor the low-affinity NGF receptor, p75, have been detected in the cortical plate (Allendoerfer et al., 1990; Chao, 1992), NGF transfection serves as a good control for any nonspecific effects of neurotrophin overexpression. Clearly, BDNF and NGF cause quantitatively different levels of dendritic

alterations. The modest changes we observed in the presence of NGF are not without precedent; NGF infusion in vivo alters the effects of monocular deprivation (Carmignoto et al., 1993), and the addition of exogenous NGF modestly alters the dendritic complexity of dendrites in cortical layers 4, 5, and 6 (McAllister et al., 1995).

Significance of BDNF-Induced Instability

Localized TrkB activation via BDNF may provide a mechanism for established neurons to undergo fine-scale remodeling in response to changes in activity levels or patterns. There is ample evidence that neurons in vivo can alter their morphology in response to changes in activity levels (Harris and Woolsey, 1979; Friedlander et al., 1982; Darian-Smith and Gilbert, 1994; Kossel et al., 1995). BDNF is well suited for influencing activity-dependent morphological changes of established architecture, since its expression levels increase in the adult (Maisonpierre et al., 1990) and because BDNF is upregulated after depolarization (Lu et al., 1991; Zafra et al., 1991), activation of voltage-sensitive calcium channels (Ghosh et al., 1994), or sensory input (Castren et al., 1992).

While it has been well documented that NGF acts as a target-derived trophic factor in the PNS (reviewed by Purves, 1988), it is less clear whether neurotrophins act in a retrograde or an anterograde fashion in the CNS. There appears to be evidence for both anterograde release from presynaptic terminals (von Bartheld et al., 1996; Altar et al., 1997) as well as retrograde targeting of BDNF to dendrites (Dugich-Djordjevic et al., 1995; Tongiorgi et al., 1997). In cortical neurons, BDNF appears to be colocalized with TrkB receptors to cell bodies and dendrites, as seen by in situ hybridization (Kokaia et al., 1993; Miranda et al., 1993). BDNF has been shown to act retrogradely (Wetmore et al., 1991) and in an autocrine fashion (Kokaia et al., 1993; Wetmore et al., 1994). Autocrine actions may be important during early development when inputs have not yet been stabilized (Miranda et al., 1993); in addition, increased levels of truncated TrkB receptors in the adult could restrict the diffusion of retrograde BDNF to a large extent (Biffo et al., 1995; Fryer et al., 1997) and thus allow only an autocrine mode of action.

Perhaps in the adult, neurons that receive novel levels or patterns of input respond by local destabilization of their dendrites and/or spines through a BDNF-dependent mechanism. This period of destabilization would allow dendrites to lose established synapses by altering the number of dendrites and increasing the turnover of spines, thereby reconfiguring the dendritic arbor to best accommodate the new pattern of input. Instead of overall increases in TrkB activation, which cause large-scale changes, local activation of TrkB receptors, either by autocrine release and action on a small portion of dendrite or by release from presynaptic terminals (von Bartheld et al., 1996; Altar et al., 1997), could restrict remodeling to just a portion of the arbor. This model could be readily tested by visualizing the actions on dendrites of highly local application of BDNF, experiments that are currently in progress.

Experimental Procedures

Slice Preparation

Coronal slices (400 μm) of P25–P28 ferret (Marshall Farms, North Rose, NY) visual cortex were prepared as previously described (Katz, 1987), except that the artificial cerebrospinal fluid (ACSF) was as follows: 140 mM NaCl, 5 mM KCl, 1 mM $MgCl_2$, 24 mM HEPES, and 1 mM $CaCl_2$. Slices were placed in 0.4 μm Millicell inserts (Millipore, Bedford, MA) within sterile 6-well plates. Media (1 ml) was placed under each insert (50% Eagle's basal medium, 25% Hanks' balanced salt solution, 25% heat-inactivated horse serum, 36 mM dextrose, 10 mM HEPES, and 100 U/ml penicillin-streptomycin; all from GIBCO BRL, Grand Island, NY). Plates were incubated in 5% CO_2 in air at 37°C for 6 hr and then at 32°C for the remaining time (20–42 hr depending on the experiment).

Particle-Mediated Gene Transfer

Cultured slices were transfected using the Helios Gene Gun (Bio-Rad, Hercules, CA) within 2 hr of slice preparation. "Bullets" were prepared in advance as described by Bio-Rad protocols. Briefly, 8 mg of 1.6 μm gold particles (Bio-Rad) were coated with DNA plasmid combinations: 16 μg epitope-tagged BDNF-myc (generous gift of Dr. E. M. Shooter) plus 8 μg pGreenlantern (GFP from GIBCO BRL), 16 μg epitope-tagged NGF-myc plus 8 μg GFP, 8 μg GFP DNA plus 16 μg pCDM8 (empty plasmid) DNA, or 16 μg GFP alone. A minimum of 30 μl each 0.05 M spermidine (Sigma, St. Louis, MO) and $CaCl_2$ were used, or this volume was increased to match the volume of DNA. Coated, rinsed gold particles were resuspended in 0.05 mg/ml polyvinylpyrrolidone (PVP) in ethanol and then loaded into tubing. Particles were accelerated into cultured slices with the gene gun pressurized to 100–120 psi of helium. Plates were returned to the incubator immediately. If the experiments called for exogenous factors such as K252a or BDNF, these were added to the media after transfection. Transfection in dual gold experiments was done as above except resuspended BDNF-myc-loaded gold particles and resuspended GFP-loaded gold particles were mixed together and then loaded into tubing.

Construction and Characterization of NGF-myc

PCDM8-NGF-myc was constructed using standard techniques. In brief, NGF-myc cDNA was cut out of the pBJ-5-NGF-myc construct (Möller et al., 1998) using restriction enzymes SacII and EcoRI, blunt-ended using T4 DNA polymerase, and subcloned into pCDM8 (Invitrogen, Carlsbad, CA), which had been cut with XhoI and filled up with T4 DNA polymerase. The function of the construct was assayed using PC12 cells. Robust neurite outgrowth was observed after transient transfection with pCDM8-NGF-myc but not after transfection with pCDM8 (data not shown).

BDNF, K252a, and TrkB-IgG

BDNF was added to a final concentration of 200 ng/ml immediately after transfection. Receptor bodies at 20 μg/ml TrkB-IgG, 20 μg/ml TrkC-IgG, or 100 μg/ml TrkC-IgG were added immediately after transfection. Receptor bodies and BDNF were generously provided by Regeneron Pharmaceuticals (Tarrytown, NY). K252a (200 nM) (Calbiochem, La Jolla, CA) in DMSO was added immediately after transfection. DMSO alone had no effect on dendritic morphology (unpublished data).

Time-Lapse Two-Photon Microscopy

Twenty-four hours after transfection, individual slices were transferred to a microscope stage by cutting the slices out of the inserts. The slices were then pinned through the insert membranes to a Sylgard-coated chamber on the stage and superfused with bicarbonate-buffered ACSF (124 mM NaCl, 1.3 mM $MgSO_4$, 3.1 mM $CaCl_2$, 5 mM KCl, 1.25 mM KH_2PO_4, 10 mM dextrose, 26 mM $NaHCO_3$) at 32°C. Our custom built two-photon microscope was assembled using Spectra-physics' (Mountain View, CA) 5 W Millenia and Titanium-Sapphire Tsunami lasers steered into a Bio-Rad MRC-500 confocal scan head. The head was mounted above an upright Zeiss Axioskop (Carl Zeiss, Thornwood, NY) and slices were viewed through a Zeiss 40× (0.75 NA) water immersion lens. An external photomultiplier tube (Hamamatsu, Bridgewater, NJ) was mounted to the camera

port for whole area detection, and Bio-Rad's COMOS software controlled data acquisition. Living neurons transfected with GFP alone or cotransfected with GFP and BDNF were repeatedly visualized using 20 mW (at the sample) of 900 nm light with a pulse width of ~80 fs at the laser. Optical sections of entire neurons were obtained at 1.0 μm steps, and images of spines were taken in 0.5 μm steps, by Kalman averaging each optical section three times. A second stack of images was taken between 4 and 18 hr later. Time between time-lapse images used for quantitation purposes ranged between 13 and 18 hr ($\bar{x}$ = 16 hr) and was called 16 hr for convenience. Care was taken to make sure that equivalent optical sections were collected in each case. All cells imaged were layer 2/3 pyramidal neurons except where noted (Figures 1A and 1B). Besides slight contrast and brightness adjustments, no image enhancement or filtering manipulations were performed on these images.

Assessing Neuronal Health and Process Filling

Repeated imaging did not induce any of the typical hallmarks of phototoxicity, such as blebbing or degeneration of dendrites, spines, or somata. These degenerative processes were evident in a small percentage of neurons in slices (both imaged and not) and did lead to cell death over time periods as short as a few hours. Therefore, sick or dying neurons would have been noticed over the time periods involved in this analysis. We have imaged neurons repeatedly, in three dimensions, for several hours with no ill effects (unpublished data). GFP filling appeared to be complete in all cases as axons could be followed for several millimeters to distinct growth cones (unpublished data). All imaged neurons were subsequently fixed and processed for immunohistochemistry using an anti-GFP antibody; despite this substantial amplification and the use of high-power oil immersion objectives, no additional processes or spines were seen that had not been observed in living neurons.

Analysis of Dendrites and Spines

Three-dimensional images and two-dimensional stacked images were opened into IPLab (Scanalytics, Fairfax, VA). Dendrites on the stacked image of the first time point were marked and counted by eye and then compared to the counted, marked dendrites on the second time point image. Somatic spines were present in both the BDNF and the control neurons, were distinguishable from dendrites on the basis of length and thickness (spines being thin and <5 μm long), and were not included in this analysis. Once marked and counted at both time points, dendrites were scored as lost or gained. Spines were essentially scored in similar ways except that only spines 3 μm or less were counted (Shepherd, 1996). This excludes dendritic filopodia, which tend to be 5–10 μm long (Ziv and Smith, 1996). To assess the appearance or disappearance of spines between the two time points, individual optical sections were examined to make sure that spines had not simply rotated in or out of view behind the dendritic shaft. Spine density measurements were calculated by dividing spine number by the measured length of imaged dendritic stretches. Pair-wise comparisons were made using Student's t test, and for multiple comparisons ANOVA was used followed by the Tukey multiple comparison test (see figure legends).

Immunohistochemistry

For visualization of GFP, BDNF-myc, NGF-myc, and BDNF expression, slices were fixed in 2.5% paraformaldehyde with 4% sucrose after imaging or after 36 hr in culture and then saturated with 30% sucrose before freeze-thawing. Blocking solution contained 2% bovine serum albumin (Boehringer Mannheim, Indianapolis, IN), 10% normal goat serum (GIBCO BRL), and 0.25% Triton (Sigma) in 0.1 M phosphate buffer. Slices were incubated with a combination of 1:2000 polycolonal rabbit antibody against GFP (Clonetech, Palo Alto, CA) and 1:1000 mouse anti-myc antibody (PharMingen, San Diego, CA). These were followed by a solution of 1:500 fluorescein-conjugated goat anti-rabbit and Cy-3-conjugated goat anti-mouse secondary antibodies (Chemicon, Temacula, CA). To visualize endogenous and transfected BDNF, slices were incubated with a 1:1000 dilution of rabbit anti-BDNF polyclonal antibody (Santa Cruz Biotechnology, Santa Cruz, CA), followed by 1:500 goat anti-rabbit Cy-3 (Chemicon). Slices were mounted, cleared with xylene, and coverslipped.

Sholl Analysis

Sholl analysis was performed using camera lucida on a Zeiss Axioplan. Using a 40× oil immersion objective (1.3 NA), the cell body was centered over a form printed with a series of concentric rings spaced an equivalent of 10 μm apart. Dendrite crossings were marked as originally described (Sholl, 1953). All cells analyzed were layer 2/3 neurons, and DAPI staining was used to assess cortical layers. To simplify the analysis and focus on the number of primary basal dendrites, only the number of intersections marked on the first ring were included in the modified Sholl analysis.

Quantification of Anti-BDNF Immunohistochemistry

Images of BDNF-stained transfected layer 2/3 neurons and untransfected layer 5 neurons were collected on a Zeiss Axioplan 2 using a 12-bit cooled CCD camera (Princeton Instruments, Trenton, NJ). Images were acquired and analyzed using IPLab (Scanalytics, Fairfax, VA) under identical parameters. To quantitate the gray values in the collected images, each cell body was defined as a region of interest (ROI) and the mean gray value within the ROI was measured. Background gray value was assessed by measuring the mean gray value in the area surrounding the soma. The corrected gray value was obtained by subtracting the background value from the cell body value.

Acknowledgments

We wish to thank Regeneron Pharmaceuticals (Tarrytown, NY) for their generous gift of BDNF, TrkB-IgG, and TrkC-IgG; Richard Mooney, Justin Crowley, Fred Horch, Ben Rubin, and Kate Winkler for their help with this manuscript; Megan Gray for technical assistance with plasmids; and Jason Goldman for his invaluable help designing and building electronics for support of the two-photon microscope. This work was supported by NIH grant EY-11553 and the Human Frontiers Science Program.

Received March 29, 1999; revised May 28, 1999.

References

Allendoerfer, K.L., Shelton, D.L., Shooter, E.M., and Shatz, C.J. (1990). Nerve growth factor receptor immunoreactivity is transiently associated with the subplate neurons of the mammalian cerebral cortex. Proc. Natl. Acad. Sci. USA *87*, 187–190.

Allendoerfer, K.L., Cabelli, R.J., Escandon, E., Kaplan, D.R., Nikolics, K., and Shatz, C.J. (1994). Regulation of neurotrophin receptors during the maturation of the mammalian visual system. J. Neurosci. *14*, 1795–1811.

Altar, C.A., Cai, N., Bliven, T., Juhasz, M., Conner, J.M., Acheson, A.L., Lindsay, R.M., and Wiegand, S.J. (1997). Anterograde transport of brain-derived neurotrophic factor and its role in the brain. Nature *389*, 856–860.

Bacon, J.P., and Murphey, R.K. (1984). Receptive fields of cricket giant interneurones are related to their dendritic structure. J. Physiol. *352*, 601–623.

Bartlett, W.P., and Banker, G.A. (1984a). An electron microscopic study of the development of axons and dendrites by hippocampal neurons in culture. I. Cells which develop without intercellular contacts. J. Neurosci. *4*, 1944–1953.

Bartlett, W.P., and Banker, G.A. (1984b). An electron microscopic study of the development of axons and dendrites by hippocampal neurons in culture. II. Synaptic relationships. J. Neurosci. *4*, 1954–1965.

Berg, M.M., Sternberg, D.W., Parada, L.F., and Chao, M.V. (1992). K-252a inhibits nerve growth factor–induced Trk proto-oncogene tyrosine phosphorylation and kinase activity. J. Biol. Chem. *267*, 13–16.

Biffo, S., Offenhäuser, N., Carter, B.D., and Barde, Y.-A. (1995). Selective binding and internalisation by truncated receptors restrict the availability of BDNF during development. Development *121*, 2461–2470.

Bourgeois, J.P., and Rakic, P. (1993). Changes of synaptic density

in the primary visual cortex of the macaque monkey from fetal to adult stage. J. Neurosci. *13*, 2801–2820.

Buchs, P.-A., and Muller, D. (1996). Induction of long-term potentiation is associated with major ultrastructural changes of activated synapses. Proc. Natl. Acad. Sci. USA *93*, 8040–8045.

Cabelli, R.J., Hohn, A., and Shatz, C.J. (1995). Inhibition of ocular dominance column formation by infusion of NT-4/5 or BDNF. Science *267*, 1662–1666.

Carmignoto, G., Canella, R., Candeo, P., Comelli, M.C., and Maffei, L. (1993). Effects of nerve growth factor on neuronal plasticity of the kitten visual cortex. J. Physiol. *464*, 343–360.

Castren, E., Zafra, F., Thoenen, H., and Lindholm, D. (1992). Light regulates expression of brain-derived neurotrophic factor mRNA in rat visual cortex. Proc. Natl. Acad. Sci. USA *89*, 9444–9448.

Chao, M.V. (1992). Neurotrophin receptors: a window into neuronal differentiation. Neuron *9*, 583–593.

Comery, T.A., Stamoudis, C.X., Irwin, S.A., and Greenough, W.T. (1996). Increased density of multiple-head dendritic spines on medium-sized spiny neurons of the striatum in rats reared in a complex environment. Neurobiol. Learn. Mem. *66*, 93–96.

Crick, F. (1982). Do dendritic spines twitch? Trends Neurosci. *5*, 44–46.

Dailey, M.E., and Smith, S.J. (1996). The dynamics of dendritic structure in developing hippocampal slices. J. Neurosci. *16*, 2983–2994.

Darian-Smith, C., and Gilbert, C.D. (1994). Axonal sprouting accompanies functional reorganization in adult cat striate cortex. Nature *368*, 737–740.

Denk, W., Strickler, J.H., and Webb, W.W. (1990). Two-photon laser scanning fluorescence microscopy. Science *248*, 73–76.

Desmond, N.L., and Levy, W.B. (1986). Changes in the postsynaptic density with long-term potentiation in the dentate gyrus. J. Comp. Neurol. *253*, 476–482.

Dugich-Djordjevic, M.M., Peterson, C., Isono, F., Ohsawa, F., Widmer, H.R., Denton, T.L., Bennett, G.L., and Hefti, F. (1995). Immunohistochemical visualization of brain-derived neurotrophic factor in the rat brain. Eur. J. Neurosci. *7*, 1831–1839.

Eysel, U.T. (1982). Functional reconnections without new axonal growth in a partially denervated visual relay nucleus. Nature *299*, 442–444.

Fifkova, E., and Delay, R.J. (1977). Long-lasting morphological changes in dendritic spines of dentate granular cells following stimulation of the entorhinal area. J. Neurocytol. *6*, 211–230.

Fischer, M., Kaech, S., Knutti, D., and Matus, A. (1998). Rapid actin-based plasticity in dendritic spines. Neuron *20*, 847–854.

Friedlander, M.J., Stanford, L.R., and Sherman, S.M. (1982). Effects of monocular deprivation on the structure–function relationship of individual neurons in the cat's lateral geniculate nucleus. J. Neurosci. *2*, 321–330.

Fryer, R.H., Kaplan, D.R., and Kromer, L.F. (1997). Truncated trkB receptors on nonneuronal cells inhibit BDNF-induced neurite outgrowth in vitro. Exp. Neurol. *148*, 616–627.

Galuske, R.A., Kim, D.S., Castren, E., Thoenen, H., and Singer, W. (1996). Brain-derived neurotrophic factor reversed experience-dependent synaptic modifications in kitten visual cortex. Suppl. Eur. J. Neurosci. *8*, 1554–1559.

Ghosh, A., Carnahan, J., and Greenberg, M.E. (1994). Requirement for BDNF in activity-dependent survival of cortical neurons. Science *263*, 1618–1623.

Goodman, L.J., Valverde, J., Lim, F., Geschwind, M.D., Federoff, H.J., Geller, A.I., and Hefti, F. (1996). Regulated release and polarized localization of brain-derived neurotrophic factor in hippocampal neurons. Mol. Cell. Neurosci. *7*, 222–238.

Harris, R.M., and Woolsey, T.A. (1979). Morphology of Golgi-impregnated neurons in mouse cortical barrels following vibrissae damage at different postnatal ages. Brain Res. *161*, 143–149.

Harris, K.M., Jensen, F.E., and Tsao, B. (1992). Three-dimensional structure of dendritic spines and synapses in rat hippocampus (CA1) at postnatal day 15 and adult ages: implications for the maturation of synaptic physiology and long-term potentiation. J. Neurosci. *12*, 2685–2705.

Hosokawa, T., Bliss, T.V., and Fine, A. (1992). Persistence of individual dendritic spines in living brain slices. Neuroreport *3*, 477–480.

Jones, T.A., Klintsova, A.Y., Kilman, V.L., Sirevaag, A.M., and Greenough, W.T. (1997). Induction of multiple synapses by experience in the visual cortex of adult rats. Neurobiol. Learn. Mem. *68*, 13–20.

Kang, H., and Schuman, E.M. (1995). Long-lasting neurotrophin-induced enhancement of synaptic transmission in the adult hippocampus. Science *267*, 1658–1662.

Kase, H., Iwahashi, K., and Matsuda, Y. (1986). K-252a, a potent inhibtor of protein kinase C from microbial origin. J. Antibiot. *39*, 1059–1065.

Katz, L.C. (1987). Local circuitry of identified projection neurons in cat visual cortex brain slices. J. Neurosci. *7*, 1223–1249.

Katz, L.C., and Constantine-Paton, M. (1988). Relationships between segregated afferents and postsynaptic neurones in the optic tectum of three-eyed frogs. J. Neurosci. *8*, 3160–3180.

Kokaia, Z., Bengzon, J., Metsis, M., Kokaia, M., Persson, H., and Lindvall, O. (1993). Coexpression of neurotrophins and their receptors in the neurons of the central nervous system. Proc. Natl. Acad. Sci. USA *90*, 6711–6715.

Kossel, A., Lowel, S., and Bolz, J. (1995). Relationships between dendritic fields and functional architecture in striate cortex of normal and visually deprived cats. J. Neurosci. *15*, 3913–3926.

Lo, D.C., McAllister, A.K., and Katz, L.C. (1994). Neuronal transfection in brain slices using particle-mediated gene transfer. Neuron *13*, 1263–1268.

Lu, B., Yokoyama, M., Dreyfus, C.F., and Black, I.B. (1991). Depolarizing stimuli regulate nerve growth factor gene expression in cultured hippocampal neurons. Proc. Natl. Acad. Sci. USA *88*, 6289–6292.

Lund, J.S., Boothe, R.G., and Lund, R.D. (1977). Development of neurons in the visual cortex (area 17) of the monkey (Macaca nemestrina): a Golgi study from fetal day 127 to postnatal maturity. J. Comp. Neurol. *176*, 149–188.

Maisonpierre, P.C., Belluscio, L., Friedman, B., Alderson, R.F., Wiegand, S.J., Furth, M.E., Lindsay, R.M., and Yancopoulos, G.D. (1990). NT-3, BDNF, and NGF in the developing rat nervous system: parallel as well as reciprocal patterns of expression. Neuron *5*, 501–509.

Maletic-Savatic, M., Malinow, R., and Svoboda, K. (1999). Rapid dendritic morphogensis in CA1 hippocampal dendrites induced by synaptic activity. Science *283*, 1923–1927.

McAllister, A.K., Lo, D.C., and Katz, L.C. (1995). Neurotrophins regulate dendritic growth in developing visual cortex. Neuron *15*, 791–803.

McAllister, A.K., Katz, L.C., and Lo, D.C. (1996). Neurotrophin regulation of cortical dendritic growth requires activity. Neuron *17*, 1057–1064.

McAllister, A.K., Katz, L.C., and Lo, D.C. (1997). Opposing roles for endogenous BDNF and NT-3 in regulating cortical dendritic growth. Neuron *18*, 767–778.

McAllister, A.K., Katz, L.C., and Lo, D.C. (1999). Neurotrophins and synaptic plasticity. Annu. Rev. Neurosci. *22*, 295–318.

Miller, M.W. (1988). Development of projection and local circuit neurons in neocortex. In Cerebral Cortex, A. Peters and E.G. Jones, eds. (New York: Plenum Press), pp. 140–147.

Miranda, R.C., Sohrabji, F., and Toran-Allerand, C.D. (1993). Neuronal colocalization of mRNAs for neurotrophins and their receptors in the developing central nervous system suggests a potential for autocrine interactions. Proc. Natl. Acad. Sci. USA *90*, 6439–6443.

Möller, C., Krüttgen, A., Heymach, J.V., Jr., Ghori, N., and Shooter, E.M. (1998). Subcellular localization of epitope-tagged neurotrophins in neuroendocrine cells. J. Neurosci. Res. *51*, 463–472.

Parnavelas, J.G., Lynch, G., Brecha, N., Cotman, C.W., and Globus, A. (1974). Spine loss and regrowth in hippocampus following deafferentation. Nature *248*, 71–73.

Purves, D. (1988). Body and Brain: A Trophic Theory of Neural Connections (Cambridge, MA: Harvard University Press).

Ruthazer, E.S., and Stryker, M.P. (1996). The role of activity in the development of long-range horizontal connections in area 17 of the ferret. J. Neurosci. *16*, 7253–7269.

Segal, M. (1995). Morphological alterations in dendritic spines of rat hippocampal neurons exposed to N-methyl-D-aspartate. Neurosci. Lett. *193*, 73–76.

Shelton, D.L., Sutherland, J., Gripp, J., Camerato, T., Armanini, M.P., Phillips, H.S., Carroll, K., Spencer, S.D., and Levinson, A.D. (1995). Human Trks: molecular cloning, tissue distribution and expression of extracellular domain immunoadhesins. J. Neurosci. *15*, 477–491.

Shepherd, G.M. (1996). The dendritic spine: a multifunctional integrative unit. J. Neurophysiol. *75*, 2197–2210.

Shimada, A., Mason, C.A., and Morrison, M.E. (1998). TrkB signaling modulates spine density and morphology independent of dendrite structure in cultured neonatal Purkinje cells. J. Neurosci. *18*, 8559–8570.

Sholl, D.A. (1953). Dendritic organization in the neurons of the visual and motor cortices of the cat. J. Anat. *87*, 387–406.

Sorra, K.E., and Harris, K.M. (1998). Stability in synapse number and size at 2 hr after long-term potentiation in hippocampal area CA1. J. Neurosci. *18*, 658–671.

Tapley, P., Lamballe, F., and Barbacid, M. (1992). K252a is a selective inhibitor of the tyrosine protein kinase activity of the Trk family of oncogenes and neurotrophin receptors. Oncogene *7*, 371–381.

Tongiorgi, E., Righi, M., and Cattaneo, A. (1997). Activity-dependent dendritic targeting of BDNF and TrkB mRNAs in hippocampal neurons. J. Neurosci. *15*, 9492–9505.

Van Harreveld, A., and Fifkova, E. (1975). Swelling of dendritic spines in the fascia dentata after stimulation of the perforant fibers as a mechanism of post-tetanic potentiation. Exp. Neurol. *49*, 736–749.

Volkmar, F.R., and Greenough, W.T. (1972). Rearing complexity affects branching of dendrites in the visual cortex of the rat. Science *176*, 1445–1447.

von Bartheld, C.S., Byers, M.R., Williams, R., and Bothwell, M. (1996). Anterograde transport of neurotrophins and axodendritic transfer in the developing visual system. Nature *379*, 830–833.

Wetmore, C., Cao, Y., Pettersson, R.F., and Olson, L. (1991). Brain-derived neurotrophic factor: subcellular compartmentalization and interneuronal transfer as visualized with anti-peptide antibodies. Proc. Natl. Acad. Sci. USA *88*, 9843–9847.

Wetmore, C., Olson, L., and Bean, A.J. (1994). Regulation of brain-derived neurotrophic factor (BDNF) expression and release from hippocampal neurons is mediated by non-NMDA type glutamate receptors. J. Neurosci. *14*, 1688–1700.

Wu, G.Y., and Cline, H.T. (1998). Stabilization of dendritic arbor structure in vivo by CaMKII. Science *279*, 222–226.

Zafra, F., Castren, E., Thoenen, H., and Lindholm, D. (1991). Interplay between glutamate and gamma-aminobutyric acid transmitter systems in the physiological regulation of brain-derived neurotrophic factor and nerve growth factor synthesis in hippocampal neurons. Proc. Natl. Acad. Sci. USA *88*, 10037–10041.

Ziv, N.E., and Smith, S.J. (1996). Evidence for a role of dendritic filopodia in synaptogenesis and spine formation. Neuron *17*, 91–102.

Note Added in Proof

Further evidence for changes in spine density after induction of long-term potentiation has recently been published: Engert, F., and Bonhoeffer, T. (1999). Dendritic spine changes associated with hippocampal long-term synaptic plasticity. Nature *399*, 66–70.